

**Title:** Evaluation of bone loss in antibacterial coated dental implants: an experimental study in dogs

**Authors names:**

Maria Godoy-Gallardo<sup>a</sup>, Maria Cristina Manzanares-Céspedes<sup>b</sup>, Pablo Sevilla<sup>c</sup>, José Nart<sup>d</sup>, Norberto Manzanares<sup>e</sup>, José M. Manero<sup>f,g</sup>, Francisco Javier Gil<sup>hi</sup>, Steven K. Boyd<sup>i</sup>, Daniel Rodríguez<sup>f,g</sup>

**Affiliations:**

<sup>a</sup> Department of Micro- and Nanotechnology, Technical University of Denmark, Kongens Lyngby, Denmark

<sup>b</sup> Unidad de Anatomía y Embriología Humana, Faculty of Dentistry, University of Barcelona, Barcelona, Spain

<sup>c</sup> Department of Mechanics, Escola Universitària Salesiana de Sarrià (EUSS), Barcelona, Spain

<sup>d</sup> Department of Periodontology, School of Dentistry, Universitat Internacional de Catalunya, Sant Cugat, Spain

<sup>e</sup> Unidad de Anatomía y Embriología Humana, Faculty of Dentistry, University of Barcelona, Barcelona, Spain

<sup>f</sup> Biomaterials, Biomechanics and Tissue Engineering Group, Dept. Materials Science and Metallurgical Engineering, Technical University of Catalonia (UPC-BarcelonaTECH), Barcelona, Spain

<sup>g</sup> Centre for Research in NanoEngineering (CRNE), UPC-BarcelonaTECH, Barcelona, Spain

<sup>h</sup> Universitat Internacional de Catalunya, Sant Cugat, Spain.

<sup>i</sup> McCaig Institute for Bone and Joint Health. University of Calgary, Calgary, Alberta, Canada.

**Corresponding author:** Daniel Rodríguez

ETSEIB-UPC - Department of Materials Science and Metallurgical Engineering

Av. Diagonal 647, 08028 – Barcelona (Spain)

Phone: +34 934010711 / Fax: +34 934016706

[daniel.rodriiguez.rius@upc.edu](mailto:daniel.rodriiguez.rius@upc.edu)

**Abstract**

The aim of this study was to evaluate the *in vivo* effect of antibacterial modified dental implants in the first stages of peri-implantitis. Thirty dental implants were inserted in the mandibular premolar sites of 5 beagle dogs. Sites were randomly assigned to Ti (untreated implants, 10 units), Ti\_Ag (silver electrodeposition treatment, 10 units), and Ti\_TSP (silanization treatment, 10 units). Coated implants were characterized by scanning electron microscopy, interferometry and X-ray photoelectron spectroscopy. Two months after implant insertion, experimental peri-implantitis was initiated by ligature placement. Ligatures were removed 2 months later, and plaque formation was allowed for 2 additional months. Clinical and radiographic analyses were performed during the study. Implant-tissue samples were prepared for micro computed tomography, backscattered scanning electron microscopy, histomorphometric and histological analyses and ion release measurements. X-ray, SEM and histology images showed that vertical bone resorption in treated implants was lower than in the control group ( $P < 0.05$ ). This effect is likely due to the capacity of the treatments to reduce bacteria colonization on the implant surface. Histological analysis suggested an increase of peri-implant bone formation on silanized implants. However, the short post-ligature period was not enough to detect differences in clinical parameters among implant groups. Within the limits of this study, antibacterial surface treatments have a positive effect against bone resorption induced by peri-implantitis.

**Keywords:** Antibacterial coating; dental implants; *in vivo*; peri-implantitis; silver electrodeposition; TESPSA

## 1. Introduction

Peri-implantitis is an inflammatory disease that affects soft and hard tissues around dental implants and is characterized by bleeding upon probing and progressive peri-implant bone loss [1,2]. If left untreated, it may cause progressively increased implant mobility and eventually implant failure. Peri-implantitis inflammatory reactions have been detected in about 10 to 45% of dental implants within 10 years after implantation [3]. Therefore, peri-implantitis creates a persistent clinical problem without an easy treatment [4].

Bacterial biofilm can be decisive in the formation and progression of peri-implantitis, so inhibiting or decreasing the bacterial colonization of the implant surface in order to reduce biofilm formation is important for the treatment of peri-implantitis. Many studies have focused on the incorporation of antibacterial agents such as silver on titanium surfaces. Silver and silver-based compounds are highly effective at inhibiting bacteria growth [5] as they damage the DNA of both Gram-positive and Gram-negative bacteria [6]. Different techniques have been explored to add silver in different states to titanium surfaces (e.g., ion implantation [7], physical vapor deposition (PVD) [8], magnetron sputtering [9] and micro arc oxidation [10]). Another strategy to confer antibacterial properties to titanium surfaces involves using silanes as an anchoring platform for active molecules with different effects on cells and bacteria, such as induction of cell proliferation, cell differentiation, or antibacterial properties. Silanes may also induce such biological effects by themselves. In a previous study, the antibacterial effect of TESPSA silane was detected *in vitro* when compared to control and surface-treated titanium samples without eliciting cytotoxic effects on human cells [11].

Antibacterial coatings may significantly influence the progress of peri-implantitis. Different antibacterial coatings have been tested *in vitro*, achieving a decrease in biofilm formation and

bacterial adhesion. Few studies, however, have provided *in vivo* information on the early effect on peri-implantitis of antibacterial coatings of dental implants [12,13]. Most studies have focused on the effect of bonding antibiotics [14,15] or antiseptic molecules [16] onto the implant surface. Other investigations were based on doping titanium with a photosensitizing surface [17], metallic ions with antibacterial properties [18] or studying the effect of distinct titanium oxide microstructures and thicknesses [13].

The hypothesis of the present study was that dental implants treated with antibacterial coatings (silver electrodeposition and 3-(triethoxysilyl)propyl succinic anhydride (TESPSA) silane) would reduce bone resorption caused by ligature-induced peri-implantitis and enhance osseointegration.

## **2. Material and Methods**

EU Directive 2010/63/EU and Spanish RD 1201/2005 regulations for the care and use of laboratory animals for scientific purposes have been observed. The protocol was approved by the Ethics Committee for Animal Research of the Rof Codina Veterinary Hospital, University of Santiago de Compostela, Spain. In order to minimize the effect of performance bias when allocating the implants in animals and assessing results, samples were identified with a code unknown by any person relevant to the study. All the details of the study are described in accordance with the ARRIVE guidelines [19].

### **2.1. Animals**

Five adult female beagle dogs about  $2.3 \pm 0.05$  years old and  $11.6 \pm 1.3$ kg were used. The number of animals was determined by considering previous studies, the 3 Rs (replacement, refinement, and reduction) for the use of animals in research and performing a sample size calculation for a statistical power of 0.9 [12,13,17,20-21]. All the animals had normal mandibles, no generalized

occlusal trauma, no viral or fungal lesions, good overall health, and no systemic compromises according to veterinary exams. During the experiment, the 5 animals were housed separately in kennels at Rof Codina Veterinary Hospital in 100% fresh air with ambient temperature of  $25\pm 0.1^{\circ}\text{C}$  and humidity of 40-70%. They were fed a soft diet twice daily and given free access to fresh water.

## **2.2. Surface treatments**

Thirty commercial dental implants with cylindrical threaded geometry (3.5mm diameter and 8mm length) were provided by Klockner (Soadco S.A., Escaldes-Engordany, Andorra). The implants are manufactured with the threaded body chemically etched and sandblasted, while the implant head is untreated (machined).

Each implant group consisted of 10 implants. Groups were coded as: (i) **Ti\_Ag**: Implants with silver electrodeposition, (ii) **Ti\_TSP**: Implants with TESPSA silanization and (iii) **Ti**: Dental implants without further processing (control group).

Electrodeposition of silver on dental implants was carried out as previously described for titanium surfaces [22,23]. Briefly, the anodizing process was controlled with a potentiostat (PARSTAT 2273, Princeton Applied Research, Oak Ridge, TN, USA) that generated a rectangular voltage pulse. The electrolyte consisted of a solution of  $\text{AgNO}_3$  0.1M and  $\text{Na}_2\text{S}_2\text{O}_3$  0.2M. The treatment was applied to the head of the implant. All implants were sonicated in ethanol, distilled water and acetone for 15 min each and dried with nitrogen.

TESPSA bonding to titanium surfaces has been described elsewhere [11]. Succinctly, dental implant surfaces were activated with 5M NaOH for 24h at  $60^{\circ}\text{C}$ . Implants were thoroughly cleaned twice by immersion in distilled water for 30 min, washed with acetone and dried with nitrogen gas. Pretreated implants were silanized with TESPSA (0.5 %, v/v) in anhydrous toluene

for 1h at 70°C in nitrogen atmosphere. The silanization was applied in a solution of 3% (v/v) N,N-diisopropylethylamine (DIEA) to maintain a basic environment. After completion of the reaction, the silanized implants were sonicated with toluene for 10 min. Afterwards, substrates were thoroughly washed with isopropanol, ethanol, distilled water, and acetone for 15 min each and dried with nitrogen. All implants were individually packaged and sterilized with ethylene oxide (Soadco S.A., Escaldes-Engordany, Andorra) and stored at room temperature.

### **2.3. Physicochemical characterization of the surfaces**

Implant surfaces were analyzed with scanning electron microscopy (SEM) (Zeiss Neon40, Carl Zeiss NTS GmbH, Oberkochen, Germany) and white-light interferometry (Wyko NT1100, Veeco Instruments, NY, USA). Surface elemental analyses (3 per group) were performed by X-ray photoelectron spectroscopy (XPS) with a Mg anode XR50 operating at 150W (D8 advance, SPECS Surface NanoAnalysis GmbH, Zurich, Switzerland). Binding energies were referred to the C 1s signal at 284.8 eV.

### **2.4. Surgical and clinical procedures**

A modified ligature-induced peri-implantitis model in beagle dogs was used, because of their likeness with human bone in relation to their size and ease of handling [20,21]. An outline of the experiment is presented in **Figure 1**. Mandibular premolars were extracted from the animals. Implant insertion surgeries were performed 3 months later. Lateral incisions were made to avoid tension in the area of implantation, and mucoperiosteal flaps were elevated on both sides of the mandible (**Figure 2**). All surgeries were done under general inhalation anesthesia with a mix of isoflurane, nitrous oxide and oxygen (5%).

Once the sites were prepared and cleaned of debris, the implants were placed with a torque wrench (maximum torque: 35Ncm) following the manufacturer's surgical guide. Six implants (2 per implant

group) were inserted in each animal mandible. A permuted random block design was used to allocate each implant position avoiding duplication of either mandible side or position for an implant group, with a total of three implants on each mandible side (**Figures 1 and 2**). Dental implants were placed non-submerged with the 1.5mm machined surface exposed above the bone crest and a minimum distance of at least 3mm between them. 2mm healing abutments (Soadco S.A.) were screwed to the implants to protect the implant connection, tissue flaps were restored and the soft tissues were sutured around each implant using resorbable sutures (Vycril 4-0, Ethicon, Johnson&Johnson, New Brunswick, NY, USA).

Post-operatively, buprenorphine HCl was administered for pain control, and amoxicillin was used to prevent infection. For the next 10 days, chlorhexidine cleaning of the surgical areas was carried out with gauze. Animals were allowed free movement, fed a soft diet, and routinely monitored for swelling, dehiscence, and infection. The remaining teeth were brushed 3 times a week, together with chlorhexidine cleansing until ligature insertions.

Two months after implant insertion, peri-implantitis was induced by placing a 4-0 silk ligature in a sub-marginal position around the head of the implant as previously described [20,24]. Oral hygiene care was stopped. Ligatures were withdrawn two months after placement.

Radiographic measurements of the progression of peri-implant vertical bone loss (primary outcome) and clinical examinations (secondary outcome) were made at 2, 3, 4, and 6 months after implant insertion and compared to the values at the insertion time (**Figure 1**) [12,13,17].

The parameters examined included probing depth (PD), mucosal recession (R), keratinized gingiva (KG), clinical attachment level (CAL), plaque index, and gingival index [12,13,17].

Data were recorded at buccal, medial, distal, and lingual sides of each dental implant. Probing

depth and clinical attachment level were evaluated using a UNC-15 periodontal probe with a probe-tip diameter of 0.4mm (Hu-Friedy GmbH, Leinmen, Germany).

Periapical digital X-rays were taken for each implant site as previously described [12]. Image analysis software (ImageJ/BoneJ) [25] was used to perform the calibration and measurements using the implant-abutment junction as a calibration and reference element. Two analysts, blinded with regard to the implant type, measured the mesial and distal marginal peri-implant bone levels for each implant.

Dogs were euthanized six months post-implantation by means of a thiopental sodium overdose (Tiobarbital Braun<sup>1</sup>, Braun Medical, Rubí, Spain) following sedation with acepromazine (Calmo Neosan<sup>1</sup>, Pfizer, Bilbao, Spain). An Oscillow GL 2000/831 (PRO-MED Instrumente GmbH, Tuttlingen, Germany) bone saw was used to extract 30 tissue samples, each containing an implant, the alveolar bone and the surrounding mucosa. The samples were kept in 5% glutaraldehyde solution buffered at pH 7.2 until laboratory processing.

## **2.5. Histomorphometric and histological analysis**

Each tissue sample was rinsed in sterile saline solution and maintained in a 10% neutral buffered formalin solution for 2 weeks for fixation. Once fixed, the samples were rinsed in running water for 1h and dehydrated in ethanol solutions of increasing concentration before embedding in glycomethacrylate (Tecnovit 7200, Heraeus Kulzer GmbH, Kulzer, Germany) with 1% peroxide benzoyl (BPO, Heraeus Kulzer GmbH). Polymerization was achieved applying yellow (2h) and blue light (4h) (Histolux, Heraeus Kulzer GmbH).

The 30 samples were analyzed by micro computed tomography (microCT) to determine implant position, bone implant contact (BIC) and bone volume/total volume (BV/TV). A  $\mu$ CT 35 (Scanco Medical AG, Brüttisellen, Switzerland) was used at 70 kVp, 114 $\mu$ A, 600-ms integration



time and 30- $\mu$ m voxel size. Thresholding (range 550-2500) and image analysis were performed with ImageJ/BoneJ software [25].

Each sample was sectioned in the bucco-lingual plane with a diamond-coated band saw with constant irrigation (Exakt 310, Exakt Apparatebau GmbH, Norderstedt, Germany). Two sections were obtained from each sample. Sections were polished, glued on SEM stubs and coated with a thin layer of carbon prior BS-SEM analysis with a Zeiss Neon40 Scanning Electron Microscope (SEM Carl Zeiss NTS GmbH, Oberkochen, Germany). Images with secondary electrons were taken all along the surface of each section at 15kV, a working distance of 9mm and magnification of 150 $\times$  and finally stitched for analysis [26]. Vertical bone resorption, BIC and bone area per total area (BAT) were measured with Quanto Implant software (Izolde AB, Uppsala, Sweden).

After BS-SEM analysis, each section was polished to a final thickness of about 100  $\mu$ m using a micro-grinding unit (Exakt, Apparatebau, Norderstedt, Germany). The tissue in the slice was stained using Goldner's Trichrome [26]. Bone and tissue resorption were then evaluated by optical microscopy with 80 $\times$  magnification (Leica AF7000, Leica microsystems, Mannheim, Germany).

## **2.6. Ion release analysis**

Blood and lymph fluid samples were extracted before implant insertion and after euthanasia. Five samples of 0.2ml were analyzed for each animal. Additionally, about 0.2g of soft tissue was extracted from the vicinity of each dental implant. The samples were digested with 1mL of HNO<sub>3</sub> (65%). After 12h, 1mL of ultrapure water was added to the digested fluid. Trace elements of Ti and Ag were directly determined in the diluted supernatant of 5 samples for each implant group by ICP-MS (Agilent 7500ce, Agilent, Santa Clara, CA, USA).

## **2.7. Statistical analysis**

Mean and standard deviation values were calculated for all variables of each group. Nonparametric statistical Kruskal-Wallis and Mann-Whitney U-tests were used to analyze the parameters evaluated ( $P < 0.05$ ). Data were analyzed with SPSS rev.20 (IBM, Jersey City, NY, USA).

## **3. Results**

### **3.1. Physicochemical characterization of the surfaces**

SEM images (**Figure 3**) showed a topographical effect after silver electrodeposition with the shape of rounded etching and silver deposits with globular morphology. These deposits were homogeneously dispersed on the implant surface and remained attached after sonication. Silanized implants exhibited a nonporous morphology due to the alkaline etching process. As expected, an increase in roughness was observed on implant surfaces after both treatments (**Table 1**) but without significant differences vs the control group.

The atomic composition of all surfaces was analyzed by means of XPS (**Table 2**). The treated samples showed an increase of carbon and nitrogen presence and a decrease in titanium and oxygen in comparison with the control group. In particular, the presence of silicon was unequivocally attributed to the presence of TESPSA on the surface of Ti\_TSP implants. Ti\_Ag implants had appreciable silver contents on their surface. These results are consistent with previous studies [11,22,23].

### **3.2. Clinical findings**

All the surgical procedures were well tolerated by the animals, and healing after implant placement was uneventful at all implant sites. Plaque formation during peri-implantitis resulted in signs of inflammation in the peri-implant mucosa and persisted after ligature removal.

The measured clinical parameters are shown in **Table 3**. A moderate rise in the probing depth was detected while the ligature was in place. Subsequently, an increase in the clinical attachment level was also observed after ligature insertion for all the implants studied. Once the ligature was removed, PD returned to pre-ligature levels for all samples except for Ti\_TSP implants. On the other hand, mucosal recession increased with a corresponding increase in CAL values. Keratinized gingiva exhibited a slow reduction as the study progressed. Plaque and gingiva index values, however, increased with ligature insertion and afterwards.

### **3.3. Histomorphometric and histological findings**

Mean BIC values measured by BS-SEM indicated significant differences for both Ti\_Ag and Ti\_TSP (**Table 4**). Likewise, an increase was observed for BAT values on the silane-treated implants compared to the control group. On the other hand, when measured with the microCT technique, both BIC and BV/TV values did not show significant differences between treated and control implants. Moreover, the mean values were higher than those measured by BS-SEM.

Radiographic analysis of the bone level around the implants was done at 0, 2, 3, 4, and 6 months after implant insertion (**Table 5**). During the healing period (the period after implant placement and before ligature removal) no significant differences were observed among groups, suggesting that the surface treatments do not have any influence in the healing of the marginal bone. Throughout the active breakdown period (after ligature placement and before ligature removal) an increase in bone resorption was measured for all experimental groups, but was more pronounced for the untreated implants. Significant differences were detected between Ti and modified surfaces (Ti\_Ag and Ti\_TSP) 6 months after implant insertion. Measurements of bone resorption and soft tissue on histology sections by BS-SEM and optical microscopy (**Table 5 and Figure 4**) further confirmed the bone resorption observed by radiographic analysis.

### 3.4. Ion release analysis

ICP-MS measurements (**Table 6**) did not detect significant systemic levels of silver or titanium (detection limit for the ICP-MS equipment was < 50ng/g for Ti and < 10ng/g for Ag) in blood or lymph fluid for any of the samples extracted before implant insertion or extracted after euthanasia. For tissue samples, however, silver was detected in the tissues around dental implants treated with silver (2392.3ng/g). Traces of titanium were also detected for all samples.

### 4. Discussion

Implant macro- and micro- design surfaces play important roles in implant–tissue interactions. Most surface modification treatments are intended to optimize the biological response by altering the surface topography or chemical properties. Many *in vivo* studies have been published regarding antibacterial treatments for metallic medical devices (e.g., K-wires [27,28] or prostheses [29]) or the effect of infection removal on already infected dental implants [30]. However, *in vivo* studies of dental implants with antibacterial surface treatments are scarce. In this study, a ligature-induced peri-implantitis model was chosen to reveal the *in vivo* effectiveness of the antibacterial properties of silver and silane surface treatments [12,13]. This work is a follow-up of previous *in vitro* studies on the antibacterial properties of both types of surfaces [11,22,23]. Godoy-Gallardo *et al.* studied and evaluated the antibacterial properties *in vitro* of both surfaces in a whole oral biofilm, reproducing the biofilm complexity found *in vivo* oral biofilms. The results obtained showed that both treated surfaces displayed a promising reduction in bacterial adhesion for multispecies biofilms. After 4 weeks of incubation the treated surfaces still showed a reduction in bacterial viability, increasing the proportion of dead bacteria through time on surfaces treated with silver or TESPSA [11].

Effectiveness of the surface treatments, with surface conditions similar to those studied *in vitro* [11,22,23] was confirmed by both SEM (**Figure 3**) and XPS (**Table 2**) analyses. SEM was used to observe the titanium surfaces after the treatments. Both processes had an important effect on morphology as the samples etched with NaOH showed a stable amorphous sodium titanate layer with a characteristic nanoporous morphology, whereas silver electrodeposition displayed round deposits which consist of silver and a rounded etching consequence of the pretreatment. XPS analyses characterized the silver electrodeposition by the presence of silver on the substrate with a larger concentration in the globular deposits, and silanization by the presence of silicon.

The thickness of the titanium oxide layer doped with silver is proportional to the applied electric potential, with an estimated thickness of 10-15 nm [31]. Previous studies measured a silane dry-layer thickness of 1.8-3.6nm [32]. Concurrently, the stability of the coatings was analyzed. All implants were cleaned thoroughly by sonication. Afterwards, the morphology was studied and compared with samples not sonicated (results not shown). Even though no measure was made of the adhesion of silver to the substrate, the deposits on silver persisted even after being challenged by sonication, suggesting a good adhesion to the substrate. No effects were observed for the silane coatings, even though they could suffer hydrolysis of the siloxane bonds. It is remarkable that even after an aggressive mechanical challenge, the capacity of the coatings to reduce the adhesion of both single biofilms and whole oral plaque was maintained [23].

Wettability and SFE are key parameters determining the adsorption of biomolecules onto surfaces and therefore controlling the adhesion of cells and bacteria. Changes in the wettability of the samples can be used to monitor the surface modification. In previous studies, it has been shown that TESPSA silane decreased the contact angle values with a significant increase of the

surface energy [11]. Silver electrodeposition, however, showed similar contact angle values compared to untreated titanium [22].

The absence of complications in the present study (no implants were lost) confirmed the *in vitro* lack of cytotoxicity. A normal bone healing and osseointegration sequence was observed for all the implants before the ligature insertion. After ligature placement, the evaluation of the clinical parameters corroborated the presence of signs of peri-implantitis infection around the dental implant, as expected for the chosen model [12,13]. The lack of a control group without ligature applied does not allow correlating ligature placement and bone loss. No statistically significant differences among groups, however, were detected in clinical parameters (**Table 3**), suggesting that differences in the infection between implant groups were not important enough to be detected by means of the measured clinical parameters.

Radiographic images were taken throughout the study for a direct determination of bone resorption around the dental implants (**Table 5 and Figure 4**). The measurements showed the existence of bone resorption around all the implants as early as 1 month after ligature placement (3 months after implant insertion). However, significant differences between treated implants and the control group were only detected 2 months after ligature removal (6 months after implantation). This result may indicate a limitation of this study, namely, that 2 months post-ligature was barely enough time for detecting differences between control and treated groups.

The differences observed in bone resorption between the implant groups in this study may arise from different causes. A more pronounced progression of peri-implantitis has been reported for implants with a rough surface than for those with a smooth surface in other studies with dogs [12,33]. In this study, even after discounting the effect of the macrotopographic features on the implant surface with a Fourier high-pass filter at 40/ $\mu\text{m}$ ,  $R_a$  is quite similar in all implant groups

(**Table 1**). Another possible cause could be that the specific experimental animal or the implant insertion position affects the results. When these variables were analyzed, however, no correlation was found between them and bone resorption. Hence, the differences observed in bone resorption (by radiography, BS-SEM and histology images) are probably a consequence of chemical modifications produced by the surface treatments.

Once the development of bone resorption was characterized, the histomorphometric parameters were analyzed. BIC and BAT were calculated, and the effect of the TESPSA silane on osseointegration was studied (**Table 4**). The measured BIC results indicated that all three surfaces osseointegrated. Both BIC and BAT values were higher for Ti\_TSP implants, and significant differences with the control surfaces were detected. The quantitative differences observed in BIC and BV/TV measurements between microCT and BS-SEM imaging could be due to image artifacts induced by titanium in the vicinity of the implant volume in the microCT reconstruction. These artifacts difficult measuring the voxel layer closest to the implant surface [34].

The concentration of titanium ions in blood and lymph observed in this study (<50ng/g) is in accordance with those reported for titanium prostheses in animal models and humans [35]. No significant differences in titanium presence in the tissues surrounding the dental implants (close to 2µg/g) were detected between the three implant groups. Our results are consistent with values reported by other studies [35], although high variability in measurements was detected. This variability can be explained by the variations of biological samples (such as different metabolisms of the animals) and the effect of different ion concentration in nearby implants. Thus, it is reasonable to assume that the studied antibacterial treatments do not disrupt the implant surface, increasing titanium ion release.

The systemic silver ion levels detected (<10ng/g) were also similar to those found in other *in vivo* studies [29]. The measured concentrations were much lower than the values accepted as normal in blood (200ng/g) due to the daily ingestion of small amounts of silver in food [36].

The silver obtained in the vicinity of silver-treated implants was 2.4 µg/g, while 0.3 µg/g was measured in tissues near the other implants. According to these values, it is reasonable to assume that the presence of silver close to Ti and Ti\_TSP implants is because of local diffusion from a nearby silver-treated implant.

Silver has bactericidal activity at concentrations as low as 35ng/g [37]. The minimal inhibitory concentration (MIC), however, depends on the studied strain and the study conditions. A MIC of 0.5 µg/g was reported for silver ions by Straub *et al* for gram-negative bacteria associated with periodontitis *in vivo* [38]. Mulley *et al* described that the MIC in LB broth was 3.6 µg/ml for *S.aureus* (strain MSSA476), 2.2 µg/ml for *P.aeruginosa* (strain PA01) and 3.3 µg/ml for *E.coli* (strain K12) [39]. Berger *et al* showed that using electrically generated silver, 16 bacterial species were inhibited *in vitro* at a concentration of 1.25 µg/ml [40]. Thus, the silver concentration measured close to silver-treated implants is within the therapeutic range for antibacterial activity. It is therefore expected that an antibacterial effect appears locally around those implants, as suggested by the reduced bone resorption measured around Ti\_Ag implants (**Table 6**).

The *in vivo* evaluation of silver toxicity is complex due to the diverse states that silver can present in tissues and also to the different technique used by researchers. Contradictory reports can be found of whether silver nanoparticles are less [41-43] or more toxic [10] than silver ions at equivalent concentrations. In the present study, silver concentration in the tissues close to silver anodized implants (2.4µg/g) is lower than reported limits of *in vitro* toxicity on mammal



cells (4µg/g) [44]. However, *in vitro* results cannot be directly transposed to *in vivo* measurements. Thus, the treated surfaces were previously tested *in vitro* for cytotoxic effects in two different human cell lines [11,22,23]. The results demonstrated inexistent or very low cytotoxicity effects. These results, combined with the fact that the histological observations of the samples did not found evidences of toxic effects on cells, suggest that the silver or silane concentrations present in the surroundings of the treated implants were not cytotoxic.

A post-hoc analysis of the statistical power of the study was calculated with the measured global effect size (0.496), resulting in a resulting statistical power of 0.63. The *a priori* estimation (0.9), coupled with the 3 Rs, led to use of five animals, with each dog receiving 6 implants. The decrease in the statistical power is a consequence of a much lower effect size in the present study compared to the previous studies used to calculate the sample size [12,13,20,21]. The most probable reason is that the time limitation in the spontaneous peri-implantitis progression after ligature removal might not have been optimal. In line with the 3 Rs, a short period of spontaneous peri-implantitis progression after ligature removal was chosen, but long enough to detect changes in bone resorption [20]. The reduced statistical power may limit the conclusions of this study. Nonetheless, the results provide sufficient preliminary evidence for the potential of using antibacterial coatings for prevention of early peri-implantitis effects on bone resorption.

The fact that the analysts knew the aim of the study (detection bias) could also be a possible limitation of this study. However, blinding was imposed on researchers regarding the types of sample that they analyzed, as well as the surgeons placing the implants (performance bias).

Another limitation of this study is the standard stain used in the histology section, which did not allow for the evaluation of soft tissue inflammation provoked by peri-implantitis. Soft tissues are also critical for the long-term implant success. Future investigations should focus on the long-

term effects of antibacterial surface treatments on bone resorption caused by peri-implantitis, combined with immunohistochemical studies of peri-implant tissues and ion release measurements.

## **5. Conclusions**

Antibacterial surface treatments with silver electrodeposition or TESPSA silane immobilization were successfully applied to dental implants and tested *in vivo* in beagle dogs in the first stages of the peri-implantitis. Peri-implant bone resorption after ligature-induced peri-implantitis was reduced in treated implants compared to untreated controls in X-ray measurements. No correlation was found between experimental animal or implant position with bone resorption. The short post-ligature period was not enough to detect differences in clinical parameters among implant groups. Histological observations of tissue sections close to TESPSA-treated implants suggested that this silane may enhance osseointegration. Both antibacterial surface treatments may be considered for further *in vivo* studies and clinical applications.

## **6. Acknowledgements**

The authors are very grateful to the team of veterinarians led by Dr. Fernando Muñoz at Rof Codina Veterinary Hospital, as well as to Dr. Borja Dehesa, Dr. Alejandro Padrós and Ms. Alba Manzanares. DR thanks Hayley Britz and Sarah L. Manske (University of Calgary) for their help and advice on performing bone microCT scans.

This work was supported by Research Grants MAT2009-12547 and MAT2012-30706 (MINECO/FEDER, UE), by Fundación Ramon Areces (XVI Concurso Nacional de Ayudas a la Investigación) and Generalitat of Catalonia (BE-DGR-2012).

## **7. References**

[1] H. Algraffe, F. Borumandi, L. Cascarini, Peri-implantitis, Br. J. Oral. Maxillofac. Surg. 50 (2012) 689-694.

- [2] N. Brogini, L.M. McManys, J.S. Hermann, R. Medina, R.K. Schenk, D. Buser, D.L. Cochran, Peri-implant inflammation defined by the implant-abutment interface, *J. Dent. Res.* 85 (2006) 473-478.
- [3] Y.C.M. de Waal, A.J. van Winkelhoff, H.J.A. Meijer, G.M. Raghoobar, E.G. Winkel, Differences in peri-implant conditions between fully and partially edentulous subjects: a systematic review, *J. Clin. Periodontol.* 40 (2013) 266-286.
- [4] T. Berglundh, N.U. Zitzmann, M. Donati, Are peri-implantitis lesions different from periodontitis lesions? *J. Clin. Periodontol.* 38 (2011) 188-202.
- [5] B.S. Atiyeh, M. Costagliola, S.N. Hayek, S.A. Dibo, Effect of silver on burn wound infection control and healing: review of the literature, *Burns. J. Int. Soc. Burn. Inj.* 33 (2007) 139-148.
- [6] Q.L. Feng, J. Wu, G.Q. Chen, F.Z. Cui, T.N. Kim, J.O. Kim, A mechanistic study of the antibacterial effect of silver ions on *Escherichia coli* and *Staphylococcus aureus*, *J. Biomed. Mater. Res.* 52 (2000) 662-668.
- [7] H. Márquez, D. Salazar, R. Rangel-Rojo, J.L. Angel-Valenzuela, G.V. Vázquez, E. Flores-Romero, L. Rodríguez-Fernández, A. Oliver, Synthesis of optical waveguides in SiO<sub>2</sub> by silver ion implantation, *Opt. Mater.* 35 (2013) 927-934.
- [8] L.A. Brook, P. Evans, H.A. Foster, M.E. Pemble, A. Steele, D.W. Sheel, H.M. Yates, Highly bioactive silver and silver/titania composite films grown by chemical vapour deposition, *J. Photochem. Photobiol. Chem.* 187 (2007) 53-63.
- [9] D.H. Song, S.B. Lee, J.G. Han, K.N. Kim, Antimicrobial silver-containing titanium oxide nanocomposite coatings by a reactive magnetron sputtering, *Thin Solid Films.* 519 (2011) 7079-7085.

- [10] B.S. Necula, Silver-based antibacterial surfaces for bone implants. PhD Thesis, Dept. BioMechanical Engineering, Faculty of Mechanical, Maritime and Materials Engineering Department, TU Delft, 2013-11-06. ISBN 9789461862334.
- [11] M. Godoy-Gallardo, J. Guillem-Marti, P. Sevilla, J.M. Manero, F.J. Gil, D. Rodríguez, Anhydride-functional silane immobilized onto titanium surfaces induces osteoblast cell differentiation and reduces bacterial adhesion and biofilm formation, *Mater. Sci. Eng. C.* 59 (2016) 24-52.
- [12] J-P. Albouy, I. Abrahamsson, L.G. Persson, T. Berglundh, Spontaneous progression of peri-implantitis at different types of implants. An experimental study in dogs. I: clinical and radiographic observations, *Clin. Oral. Implants. Res.* 19 (2008) 997-1002.
- [13] J-P. Albouy, I. Abrahamsson, T. Berglundh, Spontaneous progression of experimental peri-implantitis at implants with different surface characteristics: an experimental study in dogs, *J. Clin. Periodontol.* 39 (2012) 182-187.
- [14] V. Antoci, C.S. Adams, N.L. Hickok, I.M. Shapiro, J. Parvizi, Vancomycin bound to Ti rods reduces periprosthetic infection: preliminary study, *Clin. Orthop. Relat. Res.* 461 (2007) 88-95.
- [15] G. Schmidmaier, M. Lucke, B. Wildemann, N.P. Haas, M. Raschke, Prophylaxis and treatment of implant-related infections by antibiotic-coated implants: a review, *Injury* 37 (2006) 105-112.
- [16] T. Kaliche, J. Schierholz, U. Schlegel, T.M. Frangen, M. Koller, G. Printzen, D. Seybold, S. Klockner, G. Muhr, S. Arens, Effect on infection resistance of a local antiseptic and antibiotic coating on osteosynthesis implants: An in vitro and in vivo study, *J. Orthop. Res.* 24 (2006) 1622-1640.

- [17] J.A. Shibli, M.C. Martins, F.H. Nociti, V.G. Garcia, E. Marcantonio, Treatment of ligature-induced peri-implantitis by lethal photosensitization and guided bone regeneration: A preliminary histologic study in dogs, *J. Periodontol.* 74 (2003) 338-345.
- [18] A. Cochis, B. Azzimonti, C. Della Valle, R. Chiesa, C.R. Arciola, L. Rimondini, Biofilm formation on titanium implants counteracted by grafting gallium and silver ions, *J. Biomed. Mater. Res. Part A* 103A (2005) 1176-1187.
- [19] C. Kilkenny, The ARRIVE guidelines animal research: reporting in vivo experiments, *PLoS Biol.* 8 (2010) e1000412.
- [20] C.P. Marinello, T. Berglundh, I. Ericsson, B. Klinge, P.O. Glantz, J. Lindhe, Resolution of ligature-induced peri-implantitis lesions in the dog, *J. Clin. Periodontol.* 22 (1995) 475-479.
- [21] N.U. Zitzmann, T. Berglundh, I. Ericsson, L. Lindhe, Spontaneous progression of experimentally induced periimplantitis, *J. Clin. Periodontol.* 31 (2004) 845-849.
- [22] M. Godoy-Gallardo, A.G. Rodríguez-Hernández, L.M. Delgado, J.M. Manero, F.J. Gil, D. Rodríguez, Silver deposition on titanium surface by electrochemical anodizing process reduces bacterial adhesion of *Streptococcus sanguinis* and *Lactobacillus salivarius*, *Clin. Oral Implants Res.* 26 (2015) 1170-1179.
- [23] M. Godoy-Gallardo, A.Z. Wang, Y. Shen, J.M. Manero, F.J. Gil, D. Rodríguez, M. Haapasalo, Antibacterial coatings on titanium surfaces: a comparison study between in vitro single-species and multispecies biofilm, *ACS Appl. Mater. Interfaces.* 7 (2015) 5992-6001.
- [24] J. Lindhe, T. Berglundh, I. Ericsson, B. Liljenberg, C. Marinello, Experimental breakdown of peri-implant and periodontal tissues. A study in the beagle dog, *Clin. Oral Implants Res.* 3 (1992) 9-16.

- [25] M. Doube, M.M. Kłosowski, I. Arganda-Carreras, F. Cordelières, R.P. Dougherty, J. Jackson, B. Schmid, J.R. Hutchinson, S.J. Shefelbine, BoneJ: free and extensible bone image analysis in ImageJ. *Bone* 47(2010) 1076-1079.
- [26] C. Manresa, M. Bosch, M.C. Manzanares, P. Carvalho, J.J. Echeverría, A new standardized-automatic method for bone-to-implant contact histomorphometric analysis based on backscattered scanning electron microscopy images, *Clin. Oral Implants Res.* 25 (2014) 702-706.
- [27] M. Mehdikhani-Nahrkhalaji, M.H. Fathi, V. Mortazavi, S.B. Mousavi, B. Hashemi-Beni, S.M. Razavi, Novel nanocomposite coating for dental implant applications in vitro and in vivo evaluation, *J. Mater. Sci. Mater. Med.* 23 (2012) 485-495.
- [28] G. Jin, H. Qin, H. Cao, S. Qian, Y. Zhao, X. Peng, X. Zhang, X. Liu, P.K. Chu, Synergistic effects of dual Zn/Ag ion implantation in osteogenic activity and antibacterial ability of titanium, *Biomaterials.* 35 (2014) 7699-7713.
- [29] J. Hardes, H. Ahrens, C. Gerbert, A. Streitbuerger, H. Buerger, M. Erren, A. Günsel, C. Wedemeyer, G. Saxler, W. Winkelmann, G. Gosheger, Lack of toxicological side-effects in silver-coated megaprotheses in humans, *Biomaterials.* 28 (2007) 2869-2875.
- [30] M. Gosau, S. Hahnel, F. Schwarz, T. Gerlach, T.E. Reichert, R. Bûrgers, Effect of six different peri-implantitis disinfection methods on in vivo human oral biofilm, *Clin. Oral Implants Res.* 21 (2010) 866-872.
- [31] E. Gaul, Colouring titanium and related metals by electrochemical oxidation, *J. Chem. Educ.* 70 (1993) 176-179.
- [32] M. Godoy-Gallardo, C. Mas-Moruno, K. Yu, J.M. Manero, F.J. Gil, J.N. Kizhakkedathu, D. Rodriguez, Antibacterial properties of hLf1-11 peptide onto titanium surfaces: A comparison

study between silanization and surface initiated polymerization, *Biomacromolecules* 26 (2015) 483-496.

[33] J-P. Albouy, I. Abrahamsson, L.G. Persson, T. Berglundh, Implant surface characteristics influence the outcome of treatment of peri-implantitis: an experimental study in dogs, *J. Clin. Periodontol.* 38 (2011) 58-64.

[34] M.V. Swain, J. Xue, State of the art of Micro-CT applications in dental research, *Int. J. Oral Sci.* 1 (2009) 177-188.

[35] D. Rodríguez, F.J. Gil, J.A. Planell, E. Jorge, L. Alvarez, R. García, M. Larrea, A. Zapata, Titanium levels in rats implanted with Ti6Al4V treated samples in the absence of wear, *J. Mater. Sci. Mater. Med.* 10 (1999) 847-851.

[36] A.T. Wan, R.A. Conyers, C.J. Coombs, J.P. Masterton, Determination of silver in blood, urine, and tissues of volunteers and burn patients, *Clin. Chem.* 37 (1991) 1683-1687.

[37] Y. Okazaki, E. Gotoh, T. Manabe, K. Kobayashi, Comparison of metal concentrations in rat tibia tissues with various metallic implants, *Biomaterials.* 25 (2004) 5913-5920.

[38] A.M. Straub, J. Suvan, N.P. Lang, A. Mombelli, V. Braman, J. Massaro, P. Friden, M.S. Tonetti, Phase 1 evaluation of a local delivery device releasing silver ions in periodontal pockets: safety, pharmacokinetics and bioavailability, *J. Periodont. Res.* 36 (2001) 187-193.

[39] G. Mulley, A.T.A. Jenkins, R.N Waterfield, Inactivation of antibacterial and cytotoxic properties of silver ions by biologically relevant compounds, *PloS One* 9(4) (2014) e94409.

[40] T.J. Berger, J.A. Spadaro, S.E. Chapin, R.O. Becker, Electrically generated silver ions: quantitative effects on bacterial and mammalian cells, *Antimicrob. Agents Chemother.* 9 (1976) 357-358.

- [41] K.K. Panda, V.M.M. Achary, R. Krishnaveni, B.K. Padhi, S.N. Sarangi, S.N. Sahu, B.B. Panda, In vitro biosynthesis and genotoxicity bioassay of silver nanoparticles using plants, *Toxicol. in vitro* 25 (2011) 1097-1105.
- [42] J.S. Kim, J.H. Sung, J.H. Ji, K.S. Song, J.H. Lee, C.S. Kang, I.J. Yu, In vivo genotoxicity of silver nanoparticles after 90-day silver nanoparticle inhalation exposure, *Saf. Health Work* 2 (2011) 34-38.
- [43] B.K. Gaiser, T.F. Fernandes, M.A. Jepson, J.R. Lead, C.H. Tyler, M. Baalousha, A. Biswas, G.J. Britton, P.A. Coles, B.D. Johnston, Y. Ju-Nam, P. Rosenkranz, T.M. Scown, V. Stone, Interspecies comparisons on the uptake and toxicity of silver and cerium dioxide nanoparticles, *Environ. Toxicol. Chem.* 21 (2012) 144-154.
- [44] J. Pratten, S.N. Nazhat, J.J. Blaker, A.R. Boccaccini, In vitro attachment of *Staphylococcus epidermidis* to surgical sutures with and without Ag-containing bioactive glass coating, *J. Biomater. Appl.* 19 (2004) 47-57.



## Figures

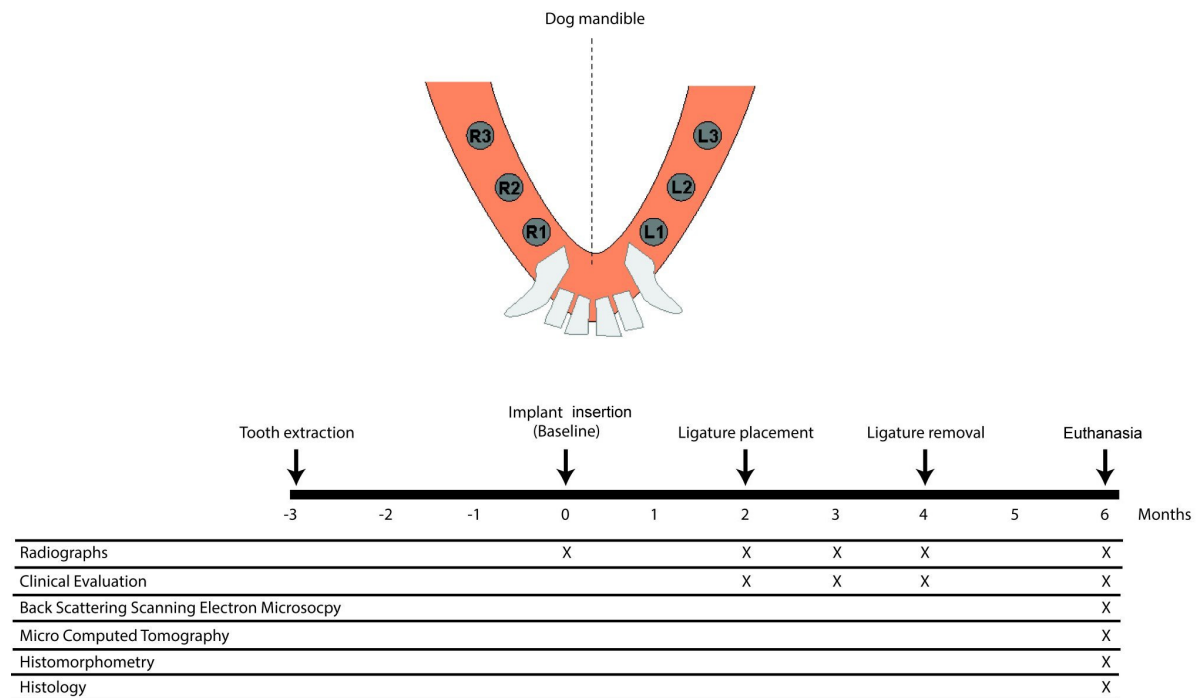


**Figure 1.** Study outline: L1-L3 and R1-R3 are the left- and right-mandible implant sites. Ligatures were placed 2 months after implant insertion and removed at month 4. Animals were euthanized 2 months later. 'X' indicates that a given analysis/evaluation was conducted at the corresponding milestone.

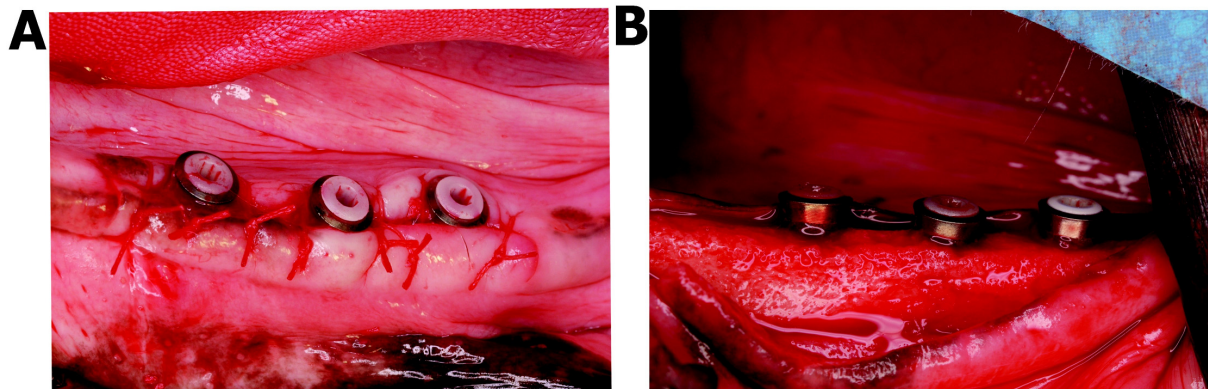


**Figure 2.** Appearance of the gingival tissue at the moment of implant placement. Three implants were installed on each side of the mandible; sutures were applied (A), and protective healing abutments were placed on the implants (B).

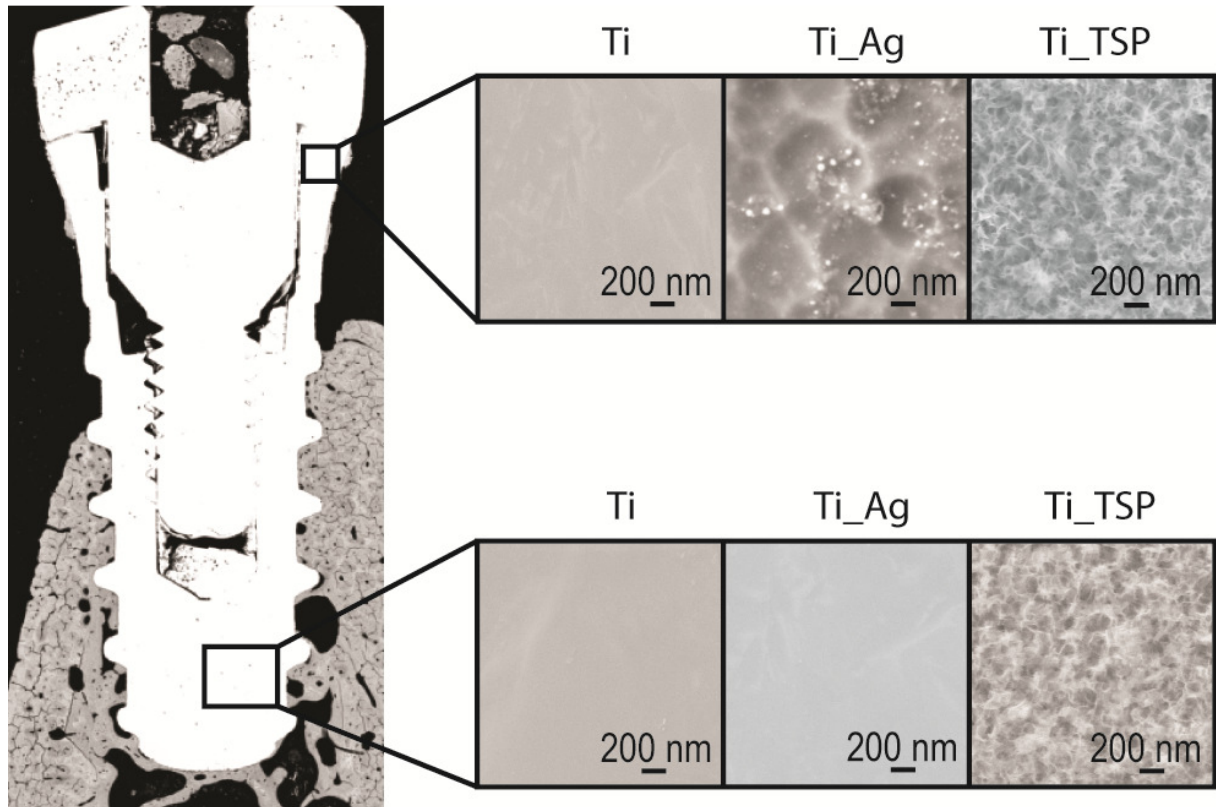


**Figure 3.** Representative BS-SEM image of a dental implant. Insets show SEM images of titanium control (Ti), silver electrodeposited implant surfaces (Ti\_Ag) and silanized implant surfaces (Ti\_TSP).

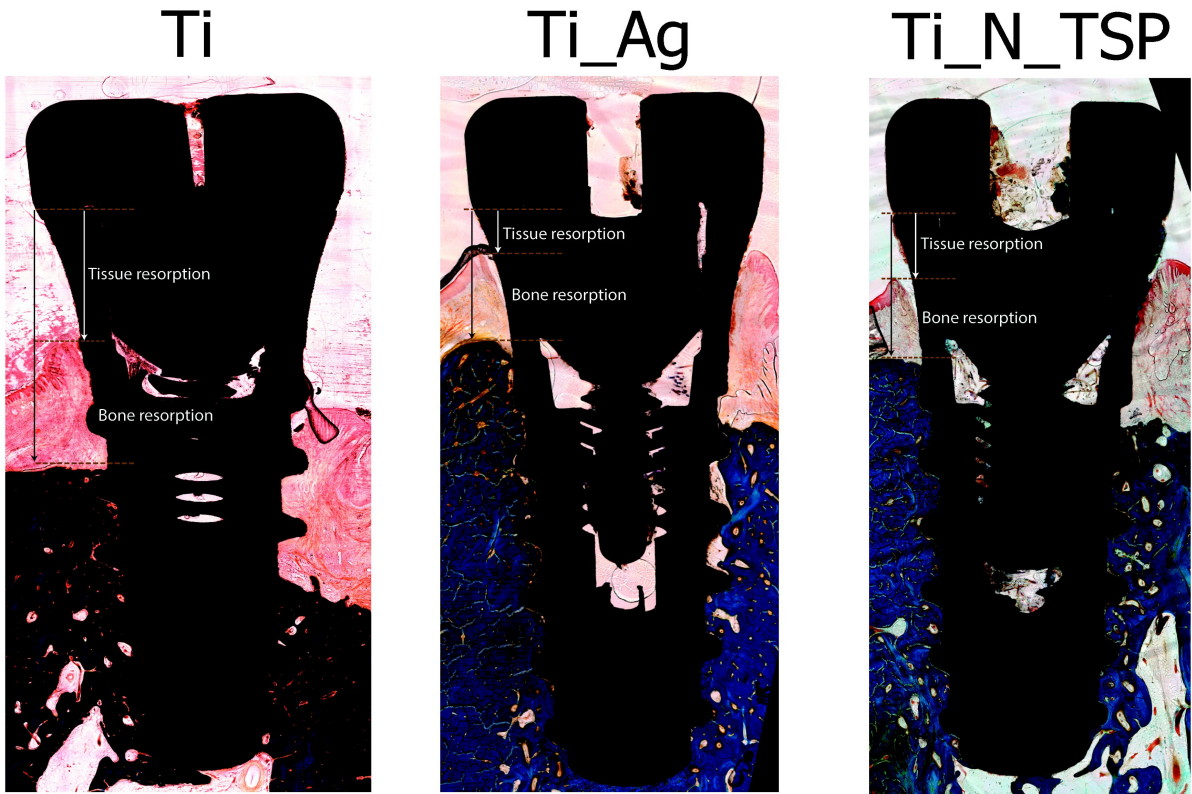


**Figure 4.** Optical microscopy image of a histological slice representative of each group of implants studied. Tissue was dyed with Goldner's Trichrome stain. Soft tissue and bone resorption measurements are shown with arrows.

**Table 1.** Roughness parameters measured for each implant group [mean  $\pm$  standard deviation].

	Unfiltered			Fourier high-band pass filter (40/mm)		
	$R_a$ (nm)	$R_{ku}$	$R_{sk}$	$R_a$ (nm)	$R_{ku}$	$R_{sk}$
<b>Ti_Ag</b>	690 $\pm$ 92	2.9 $\pm$	-0.3 $\pm$	309 $\pm$ 55	5.8 $\pm$	0.0 $\pm$ 0.1 <sup>a</sup>
<b>Ti_TSP</b>	532 $\pm$ 80	3.0 $\pm$	-0.4 $\pm$	298 $\pm$ 15	8.4 $\pm$	0.6 $\pm$ 0.2 <sup>a</sup>
<b>Ti</b>	410 $\pm$ 49	6.3 $\pm$	0.3 $\pm$ 0.1	288 $\pm$ 17	5.4 $\pm$	0.3 $\pm$ 0.1

**Table 2.** Chemical composition (atomic %) and Ag/Ti, S/Ti and Si/Ti relative atomic ratios.

	C 1s	N 1s	O 1s	S 2p	Si 2p	Ti 2p	Ag 3d	Ag/Ti	S/Ti	Si/Ti
<b>Ti_Ag</b>	47.3 $\pm$ 1.1	1.2 $\pm$ 0.2	40.1 $\pm$ 8.1	2.0 $\pm$ 0.7		6.2 $\pm$ 4.7	3.2 $\pm$ 1.0	0.6 $\pm$ 0.3	0.3 $\pm$ 0.1	
<b>Ti_TSP</b>	24.1 $\pm$ 0.7	0.8 $\pm$ 2.0	55.7 $\pm$ 0.1		5.1 $\pm$ 0.4	14.3 $\pm$ 0.4				0.4 $\pm$ 0.1
<b>Ti</b>	22.6 $\pm$ 0.3	0.9 $\pm$ 1.0	54.4 $\pm$ 0.5			22.1 $\pm$ 1.4				

**Table 3.** Mean  $\pm$  SD (mm) of probing depth (PD), mucosal recession (R), clinical attachment level (CAL), keratinized gingival (KG), plaque index, and gingival index. Statistically significant differences between measures at studied time and ligature insertion (2 months) are indicated with an “a”. Statistically significant differences between treated samples vs. control titanium are indicated with a “b” (P < 0.05) (Time is indicated as months after implant insertion).

	PD (mm)			R (mm)			CAL (mm)		
	Ti	Ti_Ag	Ti_TSP	Ti	Ti_Ag	Ti_TSP	Ti	Ti_Ag	Ti_TSP
<b>2 months</b>	1.9 $\pm$ 0.5	1.9 $\pm$ 0.5	1.9 $\pm$ 0.4	0.5 $\pm$ 0.4	0.6 $\pm$ 0.4	0.7 $\pm$ 0.5	2.4 $\pm$ 0.7	2.5 $\pm$ 0.7	2.6 $\pm$ 0.7
<b>3 months</b>	2.5 <sup>a</sup> $\pm$ 0.4	2.6 <sup>a</sup> $\pm$ 0.4	2.6 <sup>a</sup> $\pm$ 0.6	0.6 $\pm$ 0.5	0.8 $\pm$ 0.5	0.6 $\pm$ 0.8	3.1 <sup>a</sup> $\pm$ 0.5	3.4 <sup>a</sup> $\pm$ 0.5	3.2 <sup>a</sup> $\pm$ 0.7
<b>4 months</b>	2.9 <sup>a</sup> $\pm$ 0.5	2.9 <sup>a</sup> $\pm$ 0.5	2.8 <sup>a</sup> $\pm$ 0.2	0.3 <sup>a</sup> $\pm$ 0.6	0.6 <sup>a</sup> $\pm$ 0.6	0.4 <sup>a</sup> $\pm$ 0.7	3.2 $\pm$ 0.6	3.5 $\pm$ 0.6	3.2 $\pm$ 0.7
<b>6 months</b>	2.0 $\pm$ 0.8	2.1 $\pm$ 0.8	2.5 <sup>a,b</sup> $\pm$ 0.7	1.2 <sup>a</sup> $\pm$ 0.9	1.3 <sup>a</sup> $\pm$ 0.9	1.4 <sup>a</sup> $\pm$ 0.7	3.2 <sup>a</sup> $\pm$ 1.5	3.4 <sup>a</sup> $\pm$ 1.5	3.9 <sup>a</sup> $\pm$ 1.4
	KG (mm)			Plaque Index (mm)			Gingival Index (mm)		
	Ti	Ti_Ag	Ti_TSP	Ti	Ti_Ag	Ti_TSP	Ti	Ti_Ag	Ti_TSP
<b>2 months</b>	4.3 $\pm$ 0.8	3.9 $\pm$ 0.9	3.8 $\pm$ 0.9	0.7 $\pm$ 0.5	0.8 $\pm$ 0.4	0.8 $\pm$ 0.4	0.0 $\pm$ 0.0	0.0 $\pm$ 0.0	0.1 $\pm$ 0.3
<b>3 months</b>	4.0 $\pm$ 1.4	3.2 $\pm$ 1.5	3.6 $\pm$ 1.5	1.6 <sup>a</sup> $\pm$ 0.7	1.6 <sup>a</sup> $\pm$ 0.7	1.6 <sup>a</sup> $\pm$ 0.8	1.0 <sup>a</sup> $\pm$ 0.6	1.2 <sup>a</sup> $\pm$ 0.6	1.3 <sup>a</sup> $\pm$ 0.6
<b>4 months</b>	2.8 <sup>a</sup> $\pm$ 1.5	2.5 $\pm$ 1.8	2.8 $\pm$ 1.3	1.8 <sup>a</sup> $\pm$ 0.6	1.8 <sup>a</sup> $\pm$ 0.6	1.8 <sup>a</sup> $\pm$ 0.6	1.5 <sup>a</sup> $\pm$ 0.7	1.5 <sup>a</sup> $\pm$ 0.7	1.5 <sup>a</sup> $\pm$ 0.5
<b>6 months</b>	3.1 <sup>a</sup> $\pm$ 1.6	2.6 $\pm$ 1.7	2.6 $\pm$ 1.5	1.7 <sup>a</sup> $\pm$ 0.8	1.9 <sup>a</sup> $\pm$ 0.5	1.9 <sup>a</sup> $\pm$ 0.5	1.0 <sup>a</sup> $\pm$ 1.1	1.5 <sup>a</sup> $\pm$ 1.0	1.2 <sup>a</sup> $\pm$ 1.0

**Table 4.** Mean  $\pm$  SD of bone to the implant contact (%BIC) and bone area per total area (%BAT) by BS-SEM and %BIC and bone volume per total volume (%BV/TV) by microCT. Statistically significant differences between treated implants vs. titanium controls (Ti) are indicated with an “a” (P < 0.05).

	BIC(%)	BAT(%)	BIC (microCT) (%)	BV/TV (microCT) (%)
<b>Ti</b>	63.4 $\pm$ 23.4	64.6 $\pm$ 28.1	84.6 $\pm$ 10.5	84.5 $\pm$ 11.1
<b>Ti_Ag</b>	47.3 <sup>a</sup> $\pm$ 24.7	63.3 $\pm$ 23.4	81.6 $\pm$ 7.4	81.3 $\pm$ 8.0
<b>Ti_N_TSP</b>	70.6 <sup>a</sup> $\pm$ 27.4	70.6 <sup>a</sup> $\pm$ 27.4	82.5 $\pm$ 8.7	81.9 $\pm$ 9.2

**Table 5.** Mean  $\pm$  SD bone resorption (mm) measured by radiographic imaging with time measured in months after implant insertion. Mean  $\pm$  SD of distance from implant platform to the marginal bone floor measured by BS-SEM, and optical microscopy of the histological sections, and distance from implant platform to soft tissue measured with optical microscopy. Statistically significant differences between treated implants vs. titanium controls (Ti) are indicated with an “<sup>a</sup>” ( $P < 0.05$ ).

	<b>Bone X-Ray (mm)</b>					<b>Bone (BS-SEM)</b>	<b>Bone (mm) (Histology)</b>	<b>Soft tissue (mm) (Histology)</b>
	<b>0 month</b>	<b>2 months</b>	<b>3 months</b>	<b>4 months</b>	<b>6 months</b>			
<b>Ti</b>	2.1 $\pm$ 0.5	3.0 $\pm$ 0.6	3.9 $\pm$ 0.7	4.6 $\pm$ 0.7	4.9 $\pm$ 0.5	3.8 $\pm$ 0.7	3.9 $\pm$ 1.0	2.3 $\pm$ 0.6
<b>Ti_Ag</b>	2.2 $\pm$ 0.6	2.9 $\pm$ 0.6	3.5 $\pm$ 0.4 <sup>a</sup>	4.1 $\pm$ 0.5	4.4 <sup>a</sup> $\pm$ 0.5	3.2 <sup>a</sup> $\pm$ 0.5	3.2 <sup>a</sup> $\pm$ 0.7	1.9 $\pm$ 0.4
<b>Ti_N_TSP</b>	1.9 $\pm$ 0.6	2.8 $\pm$ 0.5	3.6 $\pm$ 0.5	4.0 $\pm$ 0.5 <sup>a</sup>	4.1 <sup>a</sup> $\pm$ 0.7	3.2 <sup>a</sup> $\pm$ 0.6	3.2 <sup>a</sup> $\pm$ 0.7	1.9 $\pm$ 0.7

**Table 6.** Presence of Ag and Ti as trace elements in the tissue samples (mean  $\pm$  SD). Statistically significant differences between Ti\_Ag samples vs. Ti plus Ti\_N\_TSP samples are indicated with an “<sup>a</sup>” ( $P < 0.05$ ).

	<b>Ti (ng/g)</b>	<b>Ag (ng/g)</b>
<b>Ti &amp; Ti_N_TSP</b>	1827.3 $\pm$ 1294.3	322.7 $\pm$ 223.1
<b>Ti_Ag</b>	2940.9 $\pm$ 2573.3	2392.3 <sup>a</sup> $\pm$ 334.1